ELSEVIER

Materials Science and Engineering A255 (1998) 148–153

MATERIALS SCIENCE & ENGINEERING A

# Effect of component crystal orientations on the cyclic stress–strain behavior of copper bicrystals

Z.F. Zhang *, Z G. Wang

*State Key Laboratory for Fatigue and Fracture of Materials, Institute of Metal Research, Academia Sinica, Shenyang, 110015, People's Republic of China*

Received 27 January 1998; received in revised form 14 April 1998

**Abstract**

Cyclic stress–strain curves (CSSCs) of some copper bicrystals with a grain boundary (GB) perpendicular to the stress axis were compared. It was found that the component crystal orientations played a decisive effect on the CSSCs of these bicrystals. The CSSC of $[\bar{5}913]\perp[\bar{5}79]$ copper bicrystal with two single slip oriented component crystals exhibited two plateau regions in the lower and higher plastic strain range, respectively. For $[\bar{1}23]\perp[\bar{3}35]$ and $[\bar{3}45]\perp[\bar{1}17]$ copper bicrystals, both with one single slip and one double slip oriented component crystals, the corresponding CSSCs only displayed one plateau region or pseudo-plateau region in the low and intermediate plastic strain range, respectively. However, the $[\bar{1}34]\perp[\bar{1}34]$ copper bicrystal with the same single-slip-oriented component crystal showed one plateau region over a wide plastic strain range in its CSSC, which was somewhat similar to the result for copper single crystal oriented for single-slip. In this paper, the effect of the component crystal orientations on the CSSCs of these copper bicrystals is discussed. 

*Keywords:* Copper bicrystal; Cyclic stress–strain curves; Component crystal orientation

## 1. Introduction

To clarify the fatigue mechanism of polycrystals, the cyclic deformation behaviors of copper single crystals have been widely investigated. It is well known that the cyclic stress–strain curve (CSSC) of a copper single crystal oriented for single slip showed three clearly defined regions [1–3]. Cheng and Laird [4] have reported that the cyclic saturation resolved shear stress was nearly independent of the crystal orientations and plastic strain amplitudes in the plateau region of CSSC for single slip oriented copper single crystal. This cyclic saturation stress was in the range of 28–30 MPa, which represented the critical resolved shear stress activating persistent slip bands (PSBs). The study on the cyclic deformation behaviors of copper single crystals oriented for double slip was relatively insufficient. Jin and Winter [5] have studied the cyclic stress–strain response and dislocation structures of copper single crystals oriented for double slip only at one strain amplitude ($\gamma_{pl} = 3 \times 10^{-3}$). Recently, Gong et al. [6] have investigated the CSSCs of copper single crystals ($[\bar{1}17]$ and [034]) oriented for double slip over a wide plastic strain range. It was found that the CSSC of [034] oriented single crystal only had a shorten plateau, whereas $[\bar{1}17]$ oriented crystal showed no plateau and its cyclic saturation stress increased with increasing plastic strain amplitude.

For multiple slip oriented copper single crystals, Lepisto and Kettunen [7] examined the cyclic stress–strain response of a $[\bar{1}11]$ oriented copper single crystal at a plastic strain range from $3 \times 10^{-4}$ to $2.5 \times 10^{-3}$, and found that the resolved shear stress at the end of the tests varied from 36.2 to 60.9 MPa. Recently, the cyclic deformation behavior of a [001] oriented copper single crystal have been investigated systematically by Gong et al. [8,9]. They found that its CSSC did not show any plateau behavior and followed the power law function for copper polycrystals, if modified with the Taylor factor for random texture ($M = 3.06$).

The results above indicates that the crystal orientation is a decisive factor affecting the CSSC of the copper single crystal. For polycrystals, there are two

* Corresponding author.

0921-5093/98/$ - see front matter 
*PII* S0921-5093(98)00675-3

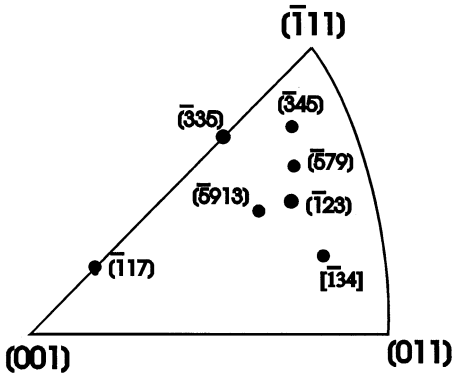


Fig. 1. The component crystal orientations of the bicrystals studied.

important factors affecting the cyclic deformation behavior, i.e. the crystal orientation and the grain boundary (GB). All the grains oriented randomly in polycrystals and GBs often lead to elastic and plastic strain inhomogeneity. Lukas and Kunz [10] suggested that there should be no plateau region in the CSSCs of copper polycrystals. By comparing the fatigue behavior of monocrystals and polycrystals, it was found that the investigation on the fatigue mechanisms of polycrystals was insufficient [11]. To clarify the difference in fatigue behavior between monocrystals and polycrystals, it is necessary to investigate the features of bicrystals. In the present study, we discuss the effect of the component crystal orientations on CSSCs of copper bicrystals with a perpendicular GB in order to have a better understanding of the cyclic deformation mechanisms of polycrystals.

## 2. Comparison of CSSCs among different copper bicrystals

The cyclic deformation behavior of different copper bicrystals with a perpendicular GB, was recently investigated by Hu and Wang [12–14] and Zhang and Wang [15,16] including $[\bar{1}23]\perp[\bar{3}35]$, $[\bar{1}34]\perp[\bar{1}34]$, $[\bar{3}45]\perp[\bar{1}17]$ and $[\bar{5}913]\perp[\bar{5}79]$ copper bicrystals. The component crystal orientations of these bicrystals are shown in Fig. 1. The results showed that these copper bicrystals had quite different CSSCs, as shown in Fig. 2. It can be seen that the $[\bar{3}45]\perp[\bar{1}17]$ bicrystal [12,13] showed a higher cyclic saturation stress than the other bicrystals. At a lower axial plastic strain range from $1.2\times10^{-4}$ to $6.3\times10^{-4}$, the cyclic saturation stress of the $[\bar{3}45]\perp[\bar{1}17]$ bicrystal increased with increasing plastic strain amplitude. However, at an axial plastic strain range from $6.3\times10^{-4}$ to $1.62\times10^{-3}$, it basically maintained a constant value of approximately 93–98 MPa, showing a pseudo-plateau region. At a higher plastic strain range, the cyclic saturation stress increased again with increasing plastic strain amplitude.

As reported by Zhang et al. [15], a $[\bar{1}23]\perp[\bar{3}35]$ copper bicrystal displayed a plateau region in its CSSC at a lower axial plastic strain range from $2.1\times10^{-4}$ to $1.1\times10^{-3}$, and the plateau axial saturation stress was approximately 65–68 MPa. When the axial plastic strain amplitude was greater than $1.1\times10^{-3}$, its cyclic saturation stress increased monotonically with the increasing plastic strain amplitude.

It is interesting to note that two plateau regions in CSSC were found for the $[\bar{5}913]\perp[\bar{5}79]$ copper bicrystal [16]. At a lower axial plastic strain range from $1.8\times$

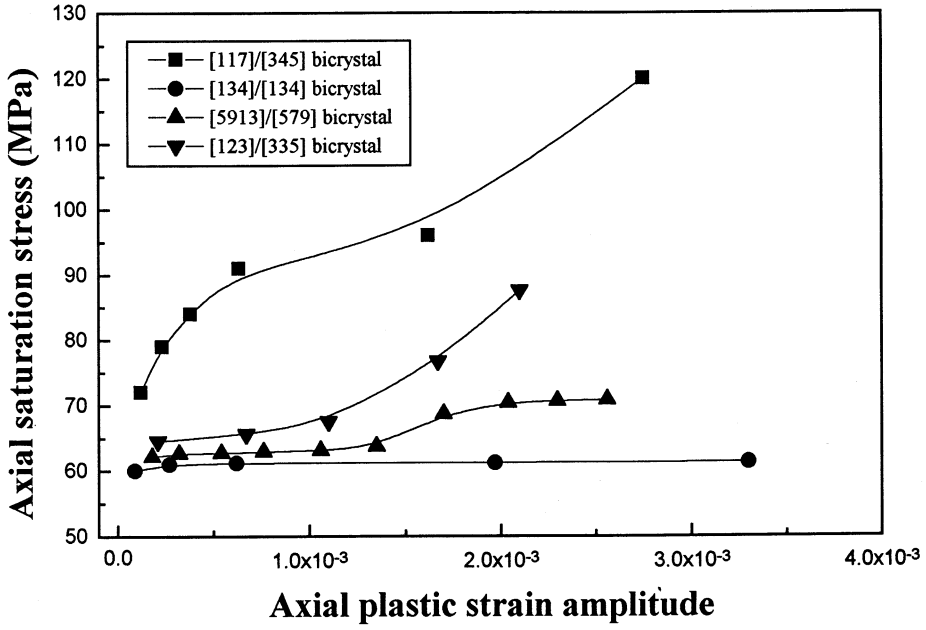


Fig. 2. The CSSCs of the copper bicrystals studied.

$10^{-4}$ to $1.35 \times 10^{-3}$, the plateau axial saturation stress was approximately 62–64 MPa. While at a higher axial plastic strain range from $1.7 \times 10^{-3}$ to $2.56 \times 10^{-3}$, the plateau axial saturation stress increased to 70–71 MPa.

Similar to the copper single crystal oriented for a single slip, the $[\bar{1}34]\perp[\bar{1}34]$ copper bicrystal [14] showed a plateau region over a very wide axial plastic strain range from $9 \times 10^{-5}$ to $3.3 \times 10^{-3}$. The plateau axial saturation stress was approximately 61–62 MPa.

## 3. Effect of component crystal orientations on CSSCs

Based on the results of copper single crystals, it has been known that the CSSCs of copper single crystals oriented for a double slip and multiple slip may or may not show a plateau region [6–9,17]. By surface observation, the slip morphology features in those copper bicrystals have been revealed [12–16]. For the $[\bar{1}34]\perp[\bar{1}34]$ and $[\bar{5}913]\perp[\bar{5}79]$ copper bicrystals, only the primary slip on each component crystal surface was activated under all the applied strain amplitudes. Fig. 3a shows the slip morphology near the grain boundary in a $[\bar{5}913]\perp[\bar{5}79]$ copper bicrystal. It can be seen that no grain boundary affected zone (GBAZ) existed. At a higher strain amplitude, the slip morphology of the bicrystal is shown in Fig. 3b and c. There is still no GBAZ and only the primary slip was activated on both component crystals G1 $[\bar{5}913]$ and G2 $[\bar{5}79]$. In particular, the plastic strains carried by the two component crystals G1 and G2 showed obvious differences, as shown in Fig. 3. That is to say, the crystal orientations play a decisive role in the determination of CSSCs. Consequently, the differences in CSSCs of the copper bicrystals above can be explained based on the combination of component crystals in the bicrystal.

Hu and Wang [12,13] attempted to compare the CSSCs between $[\bar{3}45]\perp[\bar{1}17]$ copper bicrystals and polycrystals by defining an orientation factor ($\Omega_B$) for the bicrystal as:

$$\Omega_B = \frac{\Omega_{G1} + \Omega_{G2}}{2} \quad (1)$$

Where $\Omega_{G1}$ and $\Omega_{G2}$ are the Schmid factors of the component crystals G1 and G2, respectively. They calculated the saturation resolved shear stress ($\tau_{as}$) of the copper bicrystal by the following formula:

$$\tau_{as} = \sigma_{as} \cdot \Omega_B = \sigma_{as} \cdot \frac{\Omega_{G1} + \Omega_{G2}}{2} \quad (2)$$

For the bicrystal with a perpendicular GB, the axial stresses ($\sigma_{as}$) applied on each component crystal are equal during cyclic deformation. The resolved shear stresses ($\tau_{as}^{G1}$, $\tau_{as}^{G2}$) in the primary slip direction of each component crystal will be not the same if the Schmid factors ($\Omega_{G1}$, $\Omega_{G2}$) of two component crystals are not equal. As a matter of fact, the saturation resolved shear stress ($\tau_{as}^{G1}$, $\tau_{as}^{G2}$) in the primary slip direction of each component crystal can be calculated by using the following formulae separately, i.e.:

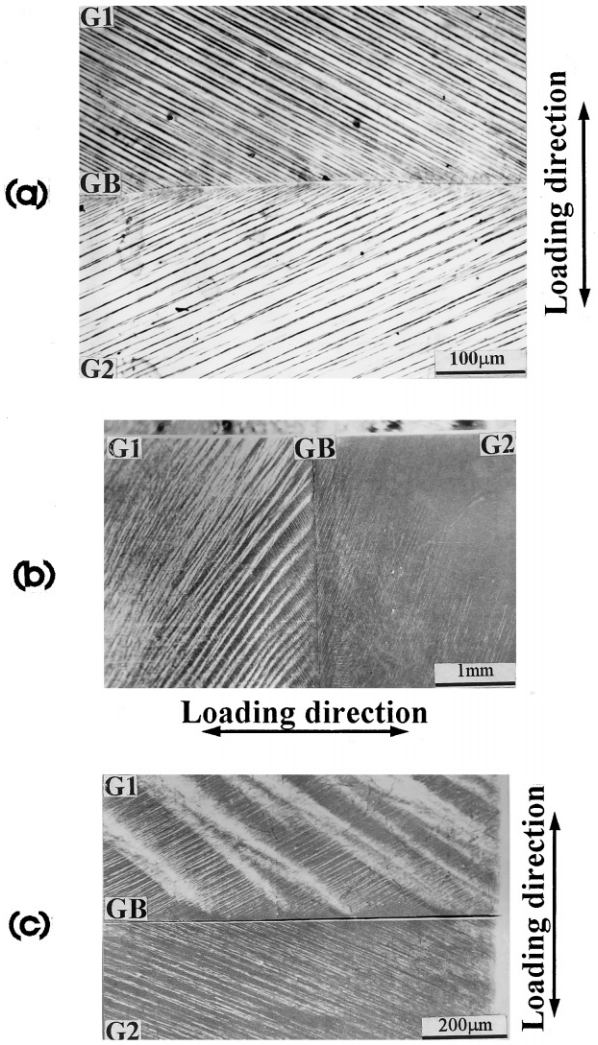


Fig. 3. Surface slip morphology of the copper bicrystal cycled at different strain amplitudes and cycles. (a) $\varepsilon_{P1} = 1.35 \times 10^{-3}$, $N = 5000$ cycles; (b) $\varepsilon_{P1} = 2.30 \times 10^{-3}$, $N = 4000$ cycles (at low magnification); (c) $\varepsilon_{P1} = 2.30 \times 10^{-3}$, $N = 4000$ cycles (at high magnification).

$$\tau_{as}^{G1} = \sigma_{as}^{B} \cdot \Omega_{G1} \quad (3)$$

$$\tau_{as}^{G2} = \sigma_{as}^{B} \cdot \Omega_{G2} \quad (4)$$

Thus, the calculated resolved shear stress ($\tau_{as}$) of the copper bicrystal by using Eq. (2), in fact, does not represent the true resolved shear stress in the primary slip direction of any component crystal. As reported by Peralta and Laird [18], the slip morphology observations above and according to Eqs. (3) and (4), the component crystal G1 with a higher Schmid factor will be subjected to a higher resolved shear stress and carry more plastic strain in the primary slip direction than the component crystal G2 with a relatively lower Schmid factor.

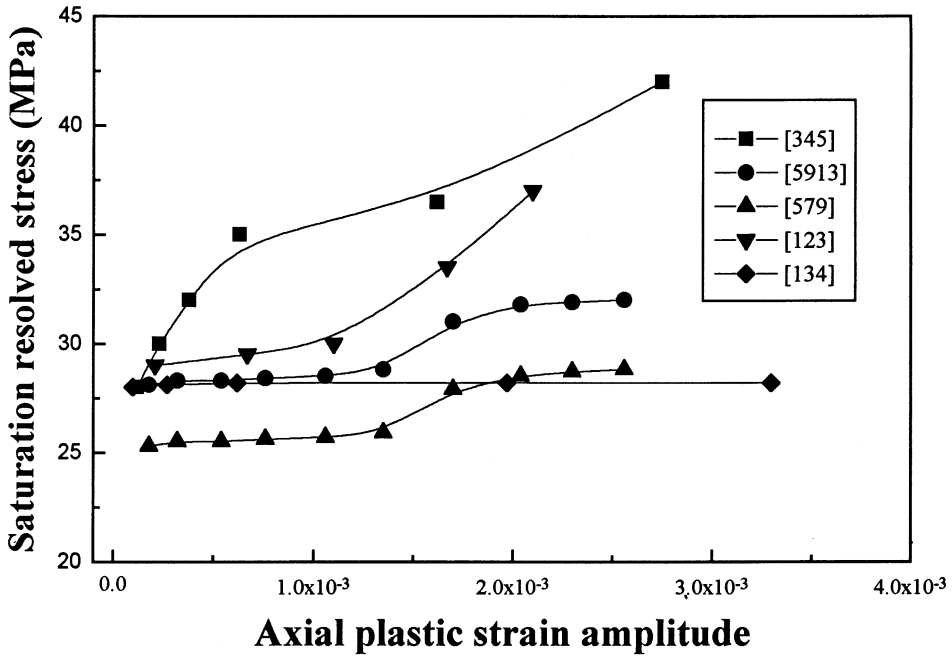


Fig. 4. The curves of the resolved shear stress of single slip oriented component crystals vs. plastic strain amplitude in the bicrystals studied.

The bicrystals discussed above contain at least one component crystal oriented for single slip. By using Eqs. (3) and (4), the cyclic saturation resolved shear stresses in the primary slip direction of the single slip oriented component crystals in these bicrystals were calculated at the applied plastic strain amplitudes. The calculated saturation resolved shear stress was plotted as a function of the applied axial plastic strain amplitude, as shown in Fig. 4. It can be seen that the resolved shear stresses in the plateau region basically maintained a constant value of approximately 28–31 MPa for [$\bar{5}$913], and [$\bar{1}$34] component crystals. However, the component crystal [$\bar{5}$79] and [$\bar{3}$45] showed a lower plateau region and an intermediate pseudo-plateau region. Apparently, the plateau (or pseudo-plateau) behavior in the cyclically deformed copper bicrystals should be attributed to the cyclic saturation of the single slip oriented component crystals at region B in their CSSCs. From the results above, we can classify these bicrystals into two types, i.e.

1. Single-single combined bicrystal, such as [$\bar{1}$34]⊥[$\bar{1}$34] and [$\bar{5}$913]⊥[$\bar{5}$79] bicrystals.
2. Single-double combined bicrystal, such as [$\bar{1}$23]⊥[$\bar{3}$35] and [$\bar{3}$45]⊥[$\bar{1}$17] bicrystals.

For the first type of bicrystals, if the Schmid factor of two component crystals are identical, such as the [$\bar{1}$34]⊥[$\bar{1}$34] bicrystal, the resolved shear stresses and plastic strains applied to each component crystal will have no difference. The CSSC of the bicrystal should display one plateau region over a wide plastic strain range such as that of a single slip oriented single crystal (Figs. 2 and 4). This argument is illustrated in Fig. 5a.

However, when the Schmid factors of two component crystals are different, as in the [$\bar{5}$913]⊥[$\bar{5}$79] bicrystal, the plastic strains and resolved shear stresses in the primary slip direction of each component crystal will be different during cyclic deformation. At a lower plastic strain range, the bulk of the plastic strain will be carried by the soft component crystal [$\bar{5}$913] with a

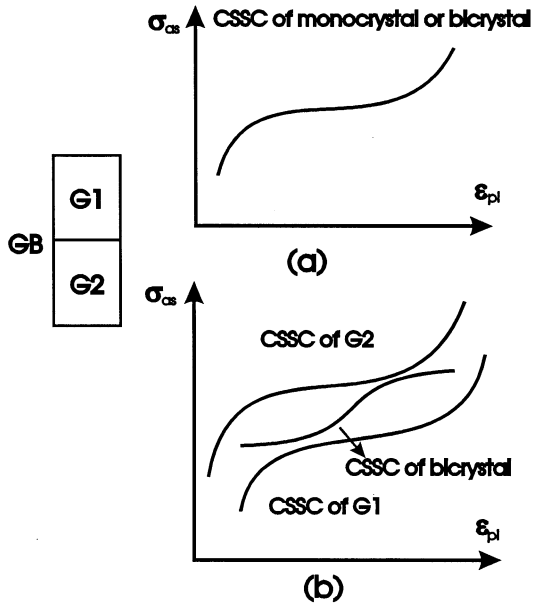


Fig. 5. The illustrations of CSSCs for the single-single combination bicrystals. (a) A diagrammatic sketch of CSSC of the component crystal [$\bar{1}$34] and the [$\bar{1}$34]⊥[$\bar{1}$34] bicrystal; (b) a diagrammatic sketch of CSSC of the component crystal [$\bar{5}$913], [$\bar{5}$79] and the [$\bar{5}$913]⊥[$\bar{5}$79] bicrystal.

relatively higher Schmid factor of 0.452. As a result, when the bicrystal cyclically saturated, the plastic strain carried by the soft component crystal [$\bar{5}$913] will be situated in region B, but the hard component crystal [$\bar{5}$79] with a relatively lower Schmid factor of 0.406 is actually deformed at the plastic stain amplitude below region B. As shown in Fig. 4, the resolved shear stresses of the component crystals G1 and G2 are 28–29 and 25–26 MPa, respectively, in the lower plateau region. It implies that the occurrence of the lower plateau region of CSSC in the [$\bar{5}$913]⊥[$\bar{5}$79] bicrystal is due to the cyclic saturation of the soft component crystal [$\bar{5}$913] at region B in its CSSC. With increasing plastic strain amplitude, the plastic strain carried by the soft component crystal [$\bar{5}$913] will reach region C in its CSSC with a greater cyclic saturation stress. As shown in Fig. 4, the resolved shear stresses of the two component crystals are 31–32 and 28–29 MPa, respectively in the upper plateau region. In this case, the plastic strain carried by the hard component crystal [$\bar{5}$79] should have reached region B of its CSSC. Dislocation observation on the cyclically saturated [$\bar{5}$913]⊥[$\bar{5}$79] copper bicrystal [16] supports the above hypothesis. The formation of a double plateau region in the CSSC of the [$\bar{5}$913]⊥[$\bar{5}$79] copper bicrystal is schematically shown in Fig. 5(b).

The argument above can also be applied to the second type bicrystals. If the Schmid factor of the single-slip oriented component crystal is higher than that of the double-slip oriented component crystal, such as the [$\bar{1}$23]⊥[$\bar{3}$35] bicrystal, the plastic strains and resolved shear stresses applied to the primary slip direction of each component crystal will also be different. In the lower axial plastic strain range from $2.1 \times 10^{-4}$ to $1.1 \times 10^{-3}$, as the bicrystal cyclically saturates, the soft [$\bar{1}$23] component crystal with a relatively higher Schmid factor of 0.467 will be cyclically deformed within region B of its CSSC with a saturation resolved shear stress of approximately 28–30 MPa (Fig. 4). However, the hard component crystal [$\bar{3}$35] with a relatively lower Schmid factor of 0.38 is subjected to a cyclic saturation below region B. As a result, the CSSC of the [$\bar{1}$23]⊥[$\bar{3}$35] bicrystal exhibited a plateau region at a lower plastic strain range. At higher strain range, the plastic strain carried by the [$\bar{1}$23] component crystal will reach region C of its CSSC. In the meantime the component crystal [$\bar{3}$35] orients double slip and its cyclic saturation stress may increase with increasing the plastic strain amplitude similar to the behavior of [001], [$\bar{1}$17] and [$\bar{1}$11] copper single crystals [6–9]. Consequently, the [$\bar{1}$23]⊥[$\bar{3}$35] bicrystal did not show an upper plateau region as the [$\bar{5}$913]⊥[$\bar{5}$79] bicrystal did at a higher plastic strain range. Fig. 6(a) schematically illustrated this situation.

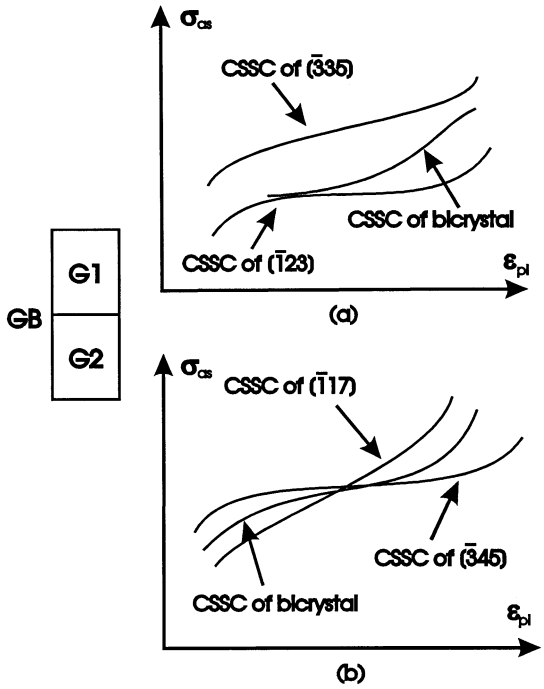


Fig. 6. The illustrations of CSSCs for the single-double combination bicrystals. (a) A diagrammatic sketch of the CSSCs of the component crystal [$\bar{1}$23], [$\bar{3}$35] and the [$\bar{1}$23]⊥[$\bar{3}$35] copper bicrystal; (b) a diagrammatic sketch of the CSSCs of the component crystal [$\bar{3}$45], [$\bar{1}$17] and the [$\bar{3}$45]⊥[$\bar{1}$17] copper bicrystal.

For the [$\bar{3}$45]⊥[$\bar{1}$17] bicrystal, the Schmid factor (0.432) of the double-slip oriented component crystal [$\bar{1}$17] is higher than that (0.390) of the single-slip oriented component crystal [$\bar{3}$45]. At a lower plastic strain range, the plastic strain carried by the [$\bar{1}$17] component crystal should be higher than that carried by the [$\bar{3}$45] component crystal. TEM observations in the [$\bar{3}$45]⊥[$\bar{1}$17] bicrystal [13] revealed that the cyclic saturation dislocations were characterized by loop patch (or vein) structures in the [$\bar{3}$45] component crystal cycled at a lower plastic strain range. Therefore, the plastic strain carried by the [$\bar{3}$45] component crystal should be in region A of its CSSC. Meanwhile, the cyclic saturation stress of the [$\bar{1}$17] copper single crystal increased with increasing strain amplitude over a wide plastic strain range [6]. As a result, the saturation stress of the [$\bar{3}$45]⊥[$\bar{1}$17] bicrystal increased with increasing plastic strain amplitude at a lower plastic strain range, as shown in Fig. 2. As the axial plastic strain was increased to $6.3 \times 10^{-4}$, the plastic strain carried by the [$\bar{3}$45] component crystal may reach region B in its CSSC and result in a plateau region in the CSSC of the [$\bar{3}$45]⊥[$\bar{1}$17] bicrystal. However, the calculated resolved shear stress of the [$\bar{3}$45] component crystal in the [$\bar{3}$45]⊥[$\bar{1}$17] bicrystal was obviously higher than 28–30 MPa and its CSSC only displayed a pseudo-plateau region, as shown in Fig. 4. This may

be associated with the operation of multiple slip systems in the $[\bar{3}45]\perp[\bar{1}17]$ bicrystal [12,13]. As a result, the $[\bar{3}45]\perp[\bar{1}17]$ bicrystal showed a higher saturation resolved shear stress at an intermediate plastic strain range than the other bicrystals. With increasing plastic strain amplitude, the saturation stress of the $[\bar{3}45]\perp[\bar{1}17]$ bicrystal will increase again because the plastic strain carried by the $[\bar{3}45]$ component crystal may reach region C in its CSSC. This process is illustrated in Fig. 6b.

## 4. Summary and conclusions

Copper bicrystals $[\bar{1}23]\perp[\bar{3}35]$, $[\bar{1}34]\perp[\bar{1}34]$, $[\bar{5}913]\perp[\bar{5}79]$ and $[\bar{3}45]\perp[\bar{1}17]$ displayed quite different CSSCs. These bicrystals can be classified into two types according to the component crystal orientations. It was found that the component crystal orientations had a decisive effect on the CSSCs of those bicrystals. In combination with the cyclic deformation behavior of copper single crystals oriented for single slip, it was concluded that the occurrence of the plateau or pseudo-plateau of their CSSCs resulted from the cyclic saturation of the single slip oriented component crystals at region B of their CSSCs.

## Acknowledgements

This work was financially supported by the National Nature Science Foundation of China(NSFC). The authors are grateful for this support.

## References

[1] J.M. Finney, C. Laird, Phil. Mag. A31 (1975) 339.
[2] H. Mughrabi, Mater. Sci. Eng. 33 (1978) 207.
[3] Z.S. Basinski, S.J. Basinski, Prog. Mater. Sci. 36 (1992) 89.
[4] A.S. Cheng, C. Laird, Mater. Sci. Eng. 51 (1981) 111.
[5] N.Y. Jin, A.T. Winter, Acta Metall. 32 (1984) 989.
[6] B. Gong, Z.G. Wang, Y.W. Zhang, Mater. Sci. Eng. A194 (1995) 171.
[7] T.K. Lepisto, P.O. Kettunen, Mater. Sci. Eng. 83 (1986) 1.
[8] B. Gong, Z.R. Wang, Z.G. Wang, Acta Mater. 45 (1997) 1365.
[9] Z.R. Wang, B. Gong, Z.G. Wang, Acta Mater. 45 (1997) 1379.
[10] P. Lukas, L. Kunz, Mater. Sci. Eng. 74 (1985) L1.
[11] P. Lukas, L. Kunz, Mater. Sci. Eng. A189 (1994) 1.
[12] Y.M. Hu, Z.G. Wang, Int. J. Fatigue 19 (1997) 59.
[13] Y.M. Hu, Z.G. Wang, Acta Mater. 45 (1997) 2655.
[14] Y.M. Hu, Z.G. Wang, S.X. Li, J. Mater. Sci. Lett. (1998) in press.
[15] Z.F. Zhang, G.Y. Li, S.D. Wu, Z.G. Wang, Proc. 8th Natl. Conf. on Fatigue, Xi'an, China, 1997, p. 74 (in Chinese).
[16] Z.F. Zhang, Z.G. Wang, Phil. Mag. A (1998) in press.
[17] X.W. Li, Z.G. Wang, G.Y. Li, S.D. Wu, S.X. Li, Acta Mater. (1998) in press.
[18] P. Peralta, C. Laird, Acta Metall. 45 (1997) 3029.